


Magnetism in frustrated Kondo and non-Kondo intermetallics: CeInCu₂ versus NdInCu₂Zhaotong Zhuang,^{1,2} Meng Lyu,¹ Te Zhang,^{1,2} Xiaoci Zhang,^{1,2} Zhen Wang,¹ Hengcan Zhao,¹ Junsen Xiang,¹ Yosikazu Isikawa³,,³ Shuai Zhang,^{1,2,4} and Peijie Sun^{1,2,4,*}¹Beijing National Laboratory for Condensed Matter Physics, Institute of Physics, Chinese Academy of Sciences, Beijing 100190, China²School of Physical Sciences, University of Chinese Academy of Sciences, Beijing 100049, China³Graduate School of Science and Engineering, University of Toyama, Toyama 930-8555, Japan⁴Songshan Lake Materials Laboratory, Dongguan, Guangdong 523808, China

(Received 1 March 2023; revised 17 May 2023; accepted 18 May 2023; published 31 May 2023)

Single crystalline intermetallics CeInCu₂ and NdInCu₂, where the rare earth ions occupy geometrically frustrated fcc lattice of Heusler-type structure, have been studied comparatively to shed light on the ground-state magnetism derived from Kondo physics and/or spin frustration competing with the Ruderman-Kittel-Kasuya-Yosida interaction. CeInCu₂ is distinct from NdInCu₂ due to the significant Kondo effect that is absent in the latter. They order antiferromagnetically at $T_N \approx 1.4$ and 2.0 K with large paramagnetic Curie-Weiss temperature of -35.4 K and -41.1 K, respectively. The electronic specific-heat coefficient $\gamma = C/T$ ($T \rightarrow 0$) = 870 mJ mol⁻¹ K⁻² in CeInCu₂ is significantly enhanced, much larger than 180 mJ mol⁻¹ K⁻² of the latter that is also enhanced albeit its non-Kondo nature. For both compounds, the Kadowaki-Woods ratio deviates greatly from the standard value expected from a Kramers doublet ground state, which, however, can be restored if one considers a smaller but still sizable γ estimated from the paramagnetic state. Likewise, the Kondo temperature of CeInCu₂ is revised to be $T_K \approx 13$ K that is double the literature values, manifesting a major effect of spin frustration to low-temperature thermodynamics beyond the Kondo physics. Similarities between the two compounds is also noticed in their temperature-field phase diagrams in spite of their thermodynamic distinctions in the thermal expansion and the Grüneisen ratio, which are much more sensitive to Kondo hybridization than to geometrical frustration.

DOI: [10.1103/PhysRevB.107.195154](https://doi.org/10.1103/PhysRevB.107.195154)**I. INTRODUCTION**

Kondo-lattice compounds represent one of the most celebrated strongly correlated matters, offering a wide variety of opportunities for emerging quantum states that are tunable by field, pressure, and chemical doping [1,2]. Here, two competing interactions are at the origin of the tunability: The on-site Kondo effect tending to screen the local moments through conduction- $4f$ (cf) electron hybridization and the intersite Ruderman-Kittel-Kasuya-Yosida (RKKY) interaction that stabilizes a magnetic order. A new tunability arising from the degree of spin frustration, which has been so far explored mainly in insulating quantum magnets, has recently added to the conventional Kondo physics and is receiving increasing attention [3,4]. This has largely expanded the spectrum of emerging quantum states at the quantum critical regime of Kondo-lattice compounds. For example, the RKKY interaction on a spin-frustrated kagome lattice competing with the Kondo effect brings about an extended quantum critical phase in CePdAl between a magnetically ordered phase and a paramagnetic heavy Fermi-liquid at absolute zero [5], instead of the more familiar quantum critical point. Enhanced quantum fluctuation in spin-frustrated Kondo lattices has been evidenced also microscopically: For example, residual

spin dynamics down to $T = 25$ mK well below its partial antiferromagnetic ordering temperature $T_N = 0.95$ K, has been observed by μ SR measurements in frustrated CePtPb [6]. Moreover, spin frustration in rare-earth contained intermetallics in the absence of significant Kondo effect becomes also a source of intriguing physics. Recent studies on HoInCu₄ reveal that half of the Ho moments remain fluctuating in the ground state with neither forming long-range order nor being Kondo compensated [7]. How the spin frustration plays its role differently in the quantum ground states in Kondo and non-Kondo intermetallics remains an interesting topic to explore.

Based on the above motivation, CeInCu₂, which crystallizes in the Heusler-type face-centered cubic (fcc) lattice came into our attention. Previous studies [8–15] have characterized it as a heavy-fermion compound with the Kondo temperature T_K of 3 – 6 K and a large electronic specific-heat coefficient $\gamma \sim 1$ J mol⁻¹ K⁻². Its magnetic order, however, had been elusive with only faint signature of ordering at temperatures ranging from below 1.1 K to 2.3 K until NMR [12,14] and neutron scattering [15] experiments became available. The latter has revealed a static short-range antiferromagnetic order below $T_N \approx 2.0$ K with a reduced moment of $\sim 0.40 \mu_B$. The crystal electric field (CEF) in cubic CeInCu₂ splits the $J = 5/2$ Hund's multiplet of Ce³⁺ into a Kramers Γ_7 ground-state doublet and an excited Γ_8 quartet at 98 K [9]. In spite of the sample-dependent and ambiguous magnetic order,

*pjsun@iphy.ac.cn

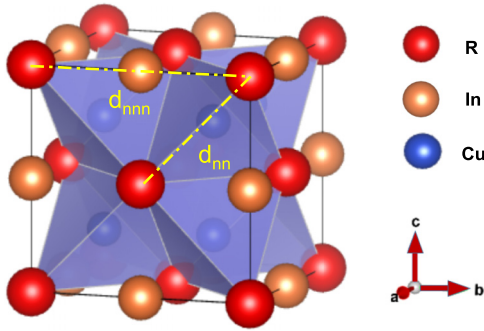


FIG. 1. Spin-frustrated Heusler-type fcc lattice of $R\text{InCu}_2$, with the tetrahedrons formed by nn R atoms highlighted.

the paramagnetic Curie temperature $\theta_p \approx -30$ K of CeInCu_2 appears to be robust [8,9]. A large value of $-\theta_p$ in cubic systems with weak crystalline anisotropy generally indicates a significant RKKY interaction via the antiferromagnetic cf coupling J ($k_B T_N \sim E_F J^2$), which is straightly associated to $T_K \sim E_F \exp^{-1/N(E_F)J}$, too, with $N(E_F)$ being the electronic density of states at the Fermi energy E_F .

The large $-\theta_p$ of CeInCu_2 reminds a similar case of CeIn_3 [16], a prototypical antiferromagnetic heavy-fermion compound crystallizing in simple cubic AuCu_3 -type structure. In CeIn_3 , $-\theta_p$ is as large as 56.5 K and, accordingly, its $T_N \approx 10.2$ K is outstandingly high despite the reduced ordered moment of $\sim 0.48 \mu_B$ [17] that resembles CeInCu_2 . Unlike the simple cubic structure of CeIn_3 , the fcc lattice of CeInCu_2 is a three-dimensional version of frustrated triangular lattice, and the antiferromagnetic interactions on the nearest-neighbor (nn) sites (Fig. 1) set up one of the oldest spin-frustrated model [18]. Indeed, neutron scattering study has confirmed the dominant nn antiferromagnetic interactions in CeInCu_2 [15]. For comparison, in this paper we have also studied the Nd-based homolog, NdInCu_2 . Previous studies have revealed an antiferromagnetic order at $T_N \approx 2$ K with a Kramers doublet ground state, too, despite its large $-\theta_p = 70$ K [8,19]. Given absence of significant Kondo effect in NdInCu_2 , the strongly enhanced ratio $|\theta_p|/T_N \approx 35$ points to even more likely spin-frustrated magnetic interactions. A comparative investigation on the similarities and distinctions between the two homologs is expected to shed general light on how spin frustration influences the low-temperature thermodynamic and transport properties in the presence of a Fermi sea, with or without significant Kondo effect.

II. EXPERIMENTS

Single crystals of CeInCu_2 and NdInCu_2 were grown by the Czochralski pulling method in an induction furnace. X-ray diffraction on a polished single-crystal facet as well as on a powdered sample obtained by grinding a piece of single crystal were recorded at room temperature for both compounds by using a Rigaku SmartLab diffractometer. A polycrystal of LaInCu_2 was also prepared by arc melting as a nonmagnetic reference. The dc magnetic susceptibility and magnetization measurements were carried out in a vibrating sample magnetometer equipped with SQUID sensor (SQUID-VSM, Quantum Design) in the temperature range

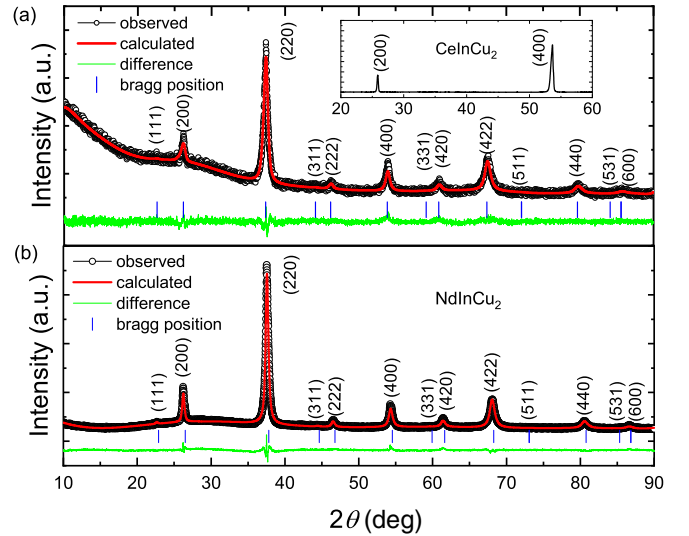


FIG. 2. Powder x-ray diffraction patterns recorded at room temperature for CeInCu_2 (a) and NdInCu_2 (b), as compared to the calculated ones. (Inset) The measured x-ray diffraction on a polished single-crystal facet of CeInCu_2 , from which the (100) plane can be readily assigned.

2–300 K, and further extended down to 0.4 K by utilizing a ^3He insert (iHelium3). The electrical resistivity was measured by using the standard four-probe method down to 0.3 K in a physical property measurement system (PPMS, Quantum Design) and an Oxford ^3He refrigerator, with electrical current applied along the crystallographic [100] axis. The specific-heat measurements were performed by the thermal-relaxation method by using PPMS ^4He specific-heat option and were extended down to 0.3 K with a homemade thermal-relaxation stage equipped on the Oxford ^3He refrigerator. Likewise, the thermal expansion was also measured down to 0.3 K by using a capacitance dilatometer in the aforementioned ^3He cryostat. All measurements in field were performed with $B \parallel [100]$. In fact, only negligible magnetic anisotropy has ever been detected for CeInCu_2 in previous paper [9].

III. EXPERIMENTAL RESULTS

Figure 2 displays the x-ray diffraction of powdered sample for CeInCu_2 (a) and NdInCu_2 (b). All the observed peaks can be indexed within the Heusler-type structure. Single crystallinity was confirmed by x-ray diffraction from a polished crystal facet (Fig. 2 inset), from which the crystal orientation is determinable. The refined lattice constants are $a = 6.8033 \text{ \AA}$ and 6.7240 \AA for CeInCu_2 and NdInCu_2 , respectively. The nearest Ce-Ce and Nd-Nd distances that constitute the edge-sharing tetrahedrons are 4.81 and 4.75 \AA (Fig. 1), slightly larger than the lattice constant and the nn Ce-Ce distance of CeIn_3 , 4.69 \AA (Ref. [16]).

The resistivity $\rho(T)$ of CeInCu_2 and NdInCu_2 , shown in Fig. 3, is characteristically different. CeInCu_2 has a broad $\rho(T)$ maximum at about 20 K, as has been previously observed in polycrystal [9]. This one-maximum behavior is most probably rooted in thermal population of the CEF states rather than phase coherence of Kondo singlets, because here T_K

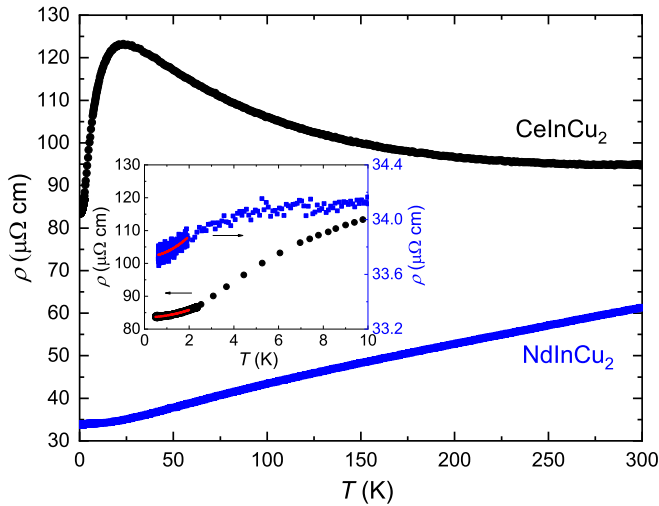


FIG. 3. Temperature-dependent resistivity $\rho(T)$ of CeInCu₂ and NdInCu₂. Inset shows the low-temperature parts with temperature-quadratic fittings at $T < 2$ K (red lines).

is much lower than the peak position. On the other hand, $\rho(T)$ of NdInCu₂ shows much reduced values and a simple metallic behavior. As shown in Fig. 3 inset, signature of magnetic ordering can hardly be resolved in $\rho(T)$ for both compounds, in line with their broadened antiferromagnetic phase transitions to be revealed below. However, the Fermi-liquid behavior following $\rho(T) = \rho_0 + AT^2$ can be simply confirmed at $T < 2$ K, with very different A values of 0.5665 and 0.0379 $\mu\Omega \text{ cm K}^{-2}$ for CeInCu₂ and NdInCu₂, respectively.

The magnetic susceptibility $\chi(T)$ measured in field cooling (FC) and zero-field cooling (ZFC) in varied fields is shown in Fig. 4(a) for CeInCu₂. A considerably broad peak is observed at ~ 1.5 K in $\chi(T)$ ($B = 0.1$ T), roughly matching the Néel temperature $T_N = 1.4$ K determined from specific heat (see below). It shifts, however, slightly to higher temperature upon increasing field, at variance with the field response of typical antiferromagnetic order. Increasing field to $B > 3$ T causes T_N to drop again and eventually fall out of the low-temperature limit (0.4 K) of our magnetic measurements. Moreover, the ZFC and FC $\chi(T)$ curves measured in $B = 0.1$ T reveal an apparent bifurcation at $T < 3$ K, which shrinks in its temperature range with field and becomes invisible at $B \geq 2$ T. The atomic disorder between Ce and In sites [13] may partially interpret the spin-glass-like behaviors, but cannot at all account for the unusual field response of the $\chi(T)$ maximum. In type-one antiferromagnetic order on the fcc lattice as revealed by neutron scattering [15], the next-nearest-neighbor (nnn) interaction is ferromagnetic competing with the spin-frustrated nn antiferromagnetic interaction. This competition provides an imperative basis to interpret the magnetic irreversibility and the field dependence of T_N .

The inverse susceptibility $\chi^{-1}(T)$ of CeInCu₂ [Fig. 4(b)] is linear-in-temperature at $T > 30$ K following the Curie-Weiss (CW) law. The effective magnetic moment $\mu_{\text{eff}}^{\text{HT}} = 2.59 \mu_B$ estimated from the CW fitting conforms to that of free Ce³⁺ ion [$g_J\sqrt{J(J+1)} = 2.54 \mu_B$ with $J = 5/2$ and $g_J = 6/7$].

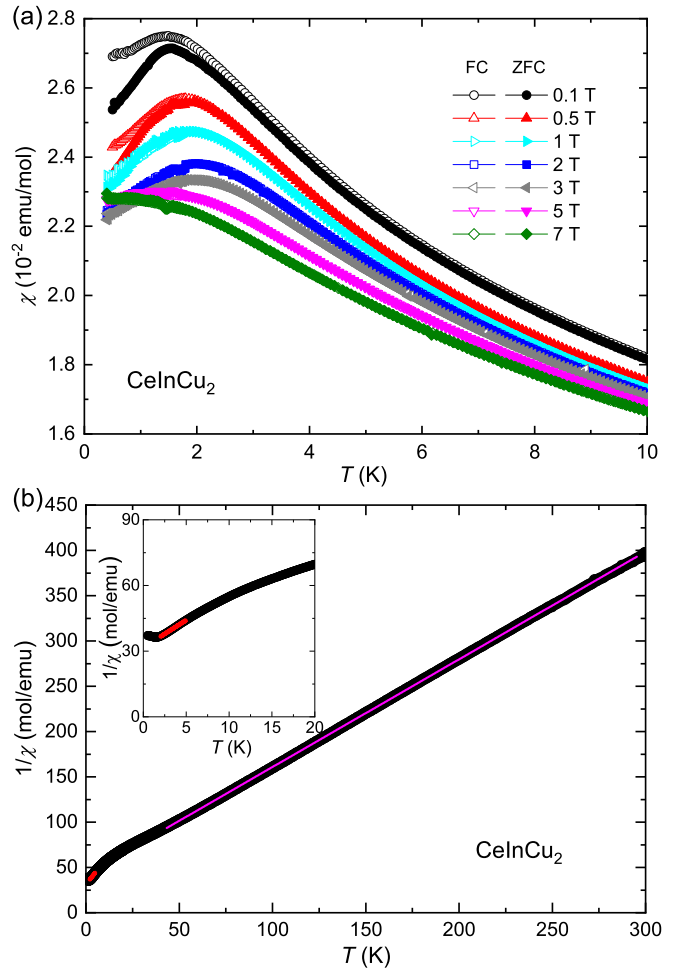


FIG. 4. (a) The magnetic susceptibility $\chi(T)$ of CeInCu₂ measured in FC and ZFC conditions in varied fields. (b) $\chi^{-1}(T)$ with the CW fittings for high- and low-temperature regions. Inset shows the low-temperature $\chi^{-1}(T)$ closeup.

As already noted, the fitting yields a significant paramagnetic Weiss temperature, $\theta_p^{\text{HT}} = -35.4$ K, and gives rise to a sizable spin-frustration ratio $f = |\theta_p^{\text{HT}}|/T_N = 25.3$. Here one should be aware that this ratio may lose part of its universality in Kondo compounds because the ordered moment is reduced due to the Kondo effect and the CEF. Alternatively, by focusing on the low enough temperatures at $T < 5$ K where the CEF Kramers ground state dominates and the CW law still applies, we obtain $\theta_p^{\text{LT}} = -12.6 (\pm 0.7)$ K and $\mu_{\text{eff}}^{\text{LT}} = 1.78 (\pm 0.04) \mu_B$ [Fig. 4(b) inset]. The latter value is larger than the effective moment of the ground-state doublet of Ce³⁺ ($\sim 1.25 \mu_B$), pointing to a likely mixing of the low-lying CEF states. By considering θ_p^{LT} that correctly accounts for the exchange interaction in the ground state, one obtains $f = |\theta_p^{\text{LT}}|/T_N = 9.0$, which remains significant and is indicative of strong spin frustration.

Compared to CeInCu₂, $\chi(T)$ ($B = 0.1$ T) of NdInCu₂ shows a narrower, but still round, peak at ~ 2.2 K [Fig. 5(a)], slightly higher than $T_N = 2.0$ K determined from specific heat (see below). Lack of $\chi(T)$ divergence at the peak evidences the existence of competing interactions, as inferred for CeInCu₂. No ZFC-FC $\chi(T)$ bifurcation can be observed,

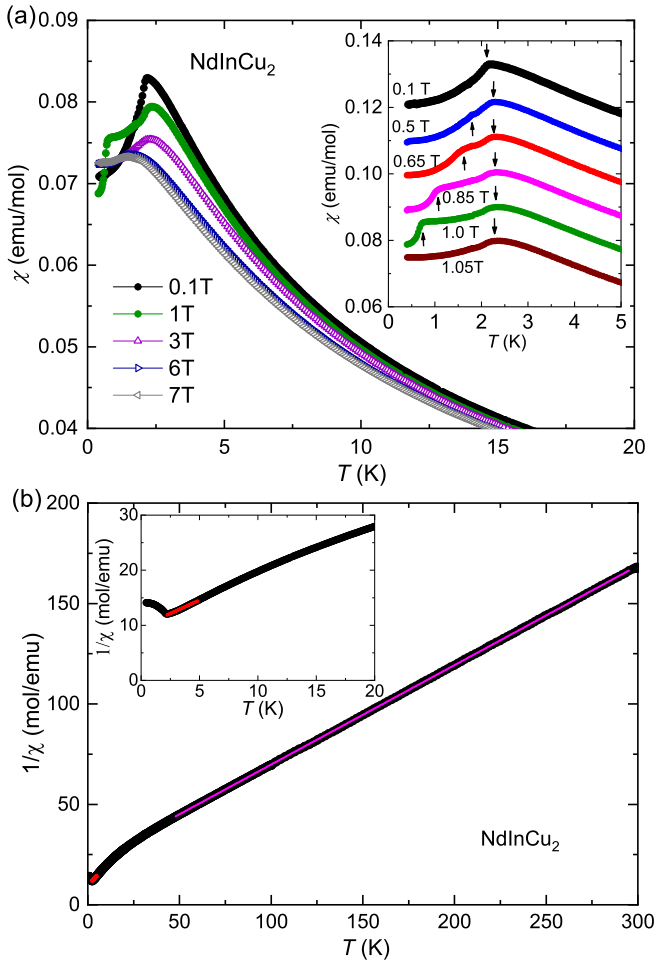


FIG. 5. (a) The magnetic susceptibility $\chi(T)$ of NdInCu₂ measured in varied fields. Inset shows the low-temperature $\chi(T)$ measured in a field window of 0.1 – 1.05 T to illustrate how the single phase transition splits into two in field, where for clarity the $\chi(T)$ curves are offset properly. (b) $\chi^{-1}(T)$ reveals a linear function of temperature following the CW law in the high-temperature range 50 – 300 K, as well as at low temperatures below about 5 K, see inset.

indicating absence of spin-glass freezing. Upon increasing field within a small window of $B \leq 1.05$ T, the round $\chi(T)$ peak splits into two anomalies with opposite field dependencies. Except for the main one that weakly increases with field indicative of ferromagnetic interaction, an additional one emerges below T_N and is drastically suppressed by field, becoming invisible for $B = 1.05$ T and above, see the downward and upward arrows in Fig. 5(a) inset. The inverse susceptibility $\chi^{-1}(T)$ of NdInCu₂ [Fig. 5(b)] follows the CW law between 50 – 300 K with $\theta_p^{\text{HT}} = -41.1$ K that is remarkable but considerably different from the literature data of a polycrystal [8]. Resembling CeInCu₂, a large spin-frustration parameter $f = |\theta_p^{\text{HT}}|/T_N = 20.6$ is obtained. The estimated effective moment in this temperature range is $4.02 \mu_B$, moderately larger than that of free Nd³⁺ ion, $g_J \sqrt{J(J+1)} = 3.62 \mu_B$ ($g_J = 8/11$; $J = 9/2$). Looking closely into the CW behavior at $T < 5$ K that is dominated by the Kramers doublet [Fig. 5(b) inset], one obtains $\theta_p^{\text{LT}} = -10.0 (\pm 0.6)$ K and

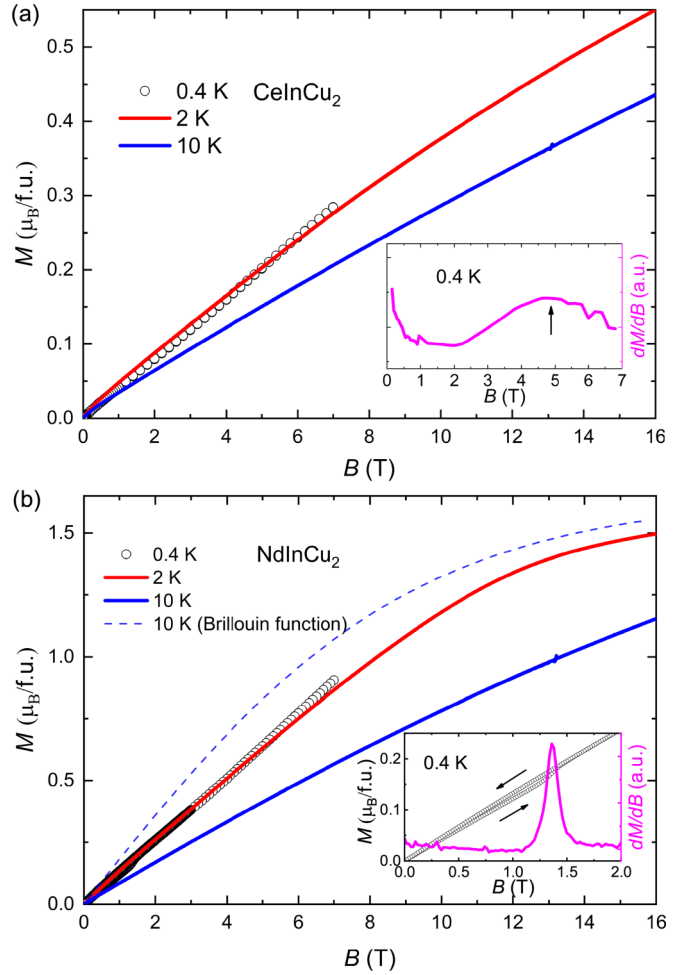


FIG. 6. Magnetization of CeInCu₂ (a) and NdInCu₂ (b) measured at three different temperatures $T = 0.4, 2,$ and 10 K. A calculation for NdInCu₂ based on the Brillouin function that models the paramagnetic response of noninteracting spins is shown in panel (b) for $T = 10$ K deep in the paramagnetic state. Inset to (a) shows dM/dB for $T = 0.4$ K, where a broad maximum appears at $B \approx 5$ T indicative of a spin-flop crossover in CeInCu₂. Inset to (b) shows the low-field closeup of $M(B)$ for NdInCu₂ and the corresponding derivative dM/dB , where a weak but clear spin-flop transition with hysteric behavior is observed.

$\mu_{\text{eff}}^{\text{LT}} = 2.87 (\pm 0.06) \mu_B$, with $f = |\theta_p^{\text{LT}}|/T_N = 5.0$ remaining sizable.

The isothermal magnetization $M(B)$ of CeInCu₂, shown in Fig. 6(a) for $T = 0.4, 2,$ and 10 K, increases almost linearly with field. $M(B)$ at the lowest temperature, $T = 0.4$ K, attains only $0.29 \mu_B$ at 7 T, significantly smaller than full moment expected for the Γ_7 Kramers doublet of Ce³⁺, $0.71 \mu_B$. The $M(B)$ measurements at 2 and 10 K were extended up to $B = 16$ T in the PPMS-VSM option, where a saturation is still unreached. Instructively, $M(B)$ of CeInCu₂ resembles not only qualitatively but quantitatively that of CeIn₃ that has a similar T_K (~ 10 K) but a much higher T_N (≈ 10.2 K) [20], suggestive of strong antiferromagnetic exchange interaction in CeInCu₂ relative to its low and obscure Néel transition. A closer look at $M(B)$ measured at $T = 0.4$ K reveals a weak spin-flop crossover that can be identified from the dM/dB

curve [see arrow in Fig. 6(a) inset]. As shown in Fig. 6(b), $M(B)$ of NdInCu₂ for $T = 2$ K reveals a clear deviation from linearity at $B > 10$ T, but does not saturate even at 16 T. $M(B)$ for 0.4 K shows a much clearer spin-flop transition (compared to that of CeInCu₂) at ~ 1.3 T, see Fig. 6(b) inset for the low-field $M(B)$ and its field derivative. Given the absence of Kondo screening in NdInCu₂ that will otherwise reduce the magnetic moment, we have computed $M(B)$ for $T = 10$ K based on the Brillouin function that characterizes the paramagnetic response of noninteracting spins [dashed line in Fig. 6(b)]. Here the effective angular momentum $J_{\text{eff}} = 1/2$ of the Kramers doublet and $g_J = 3.3$ that is experimentally derived from $\mu_{\text{eff}}^{\text{LT}} = 2.87 \mu_B$ are used. The calculated curve reveals an apparent curvature towards saturation and considerably larger magnetization values than the measured ones at 10 K. For comparison, here we mention the Nd-based antiferromagnetic NdTi₂Al₂₀ with a Kramers doublet ground state and a similar Néel temperature $T_N = 1.45$ K [21], where the isothermal magnetization measured at 0.5 K saturates already at a low field of $B \approx 1$ T. In analogy to but more transparent than the discussion made for CeInCu₂, the largely reduced magnetization of the non-Kondo NdInCu₂ in a wide field range for $T \gg T_N$ offers a piece of strong evidence for spin-frustrated antiferromagnetic interactions.

In Fig. 7(a) we show the specific heat $C(T)$ of CeInCu₂ and its nonmagnetic analog LaInCu₂. The former exhibits a broad maximum at about 2 K due to the enhanced short-range spin correlations as observed by neutron scattering [15]. Its Néel temperature $T_N = 1.4$ K is determined by the peak position of C_m/T vs T measured in zero field [Fig. 7(b)], where the magnetic part C_m is obtained by subtracting $C(T)$ of LaInCu₂ from that of CeInCu₂. The electronic specific-heat coefficient γ_{LT} estimated by linearly extrapolating C/T vs T^2 from well below T_N (in the Fermi liquid regime where T -quadratic resistivity is observed) down to absolute zero is $\sim 0.87 \text{ J mol}^{-1} \text{ K}^{-2}$, see curve I in Fig. 7(a) inset. This value is in reasonable agreement with the literature γ values [9,12,13]. Application of field suppresses T_N gradually, as expected for antiferromagnetic order and being different to the field dependence of the $\chi(T)$ peak. In the $C_m(T)$ curve [Fig. 7(b) inset], a weak hump becomes visible at $T \approx 6$ K in between the broad Néel peak and the maximum due to CEF. This is most likely a signature of the Kondo effect. In fact, similar maximum has been ever observed [9,22] but not addressed. The best fit to the hump following the Bethe ansatz calculation for spin-1/2 Kondo model [23] yields $T_K \approx 13$ K, see the red line in Fig. 7(b) inset. Alternatively, T_K estimated from $\gamma_{\text{LT}} = 0.87 \text{ J mol}^{-1} \text{ K}^{-2}$ based on the single-ion Kondo description by Rajan [24] is only ~ 6.5 K, close to the values previously reported. Apart from γ_{LT} obtained from inside the ordered phase, linearly extrapolating C/T vs T^2 from above T_N to 0 K [see Fig. 7(a) inset, curve II] yields $\gamma_{\text{HT}} = 0.23 \text{ J mol}^{-1} \text{ K}^{-2}$ for the paramagnetic phase, which is roughly one-fourth of γ_{LT} . As will be discussed below, the fourfold enhancement of γ_{LT} over γ_{HT} is considered to be mainly caused by spin frustration beyond mass renormalization of the Kondo entanglement. Therefore, evaluation of T_K based on γ_{LT} may cause a significant underestimation and $T_K = 13$ K is physically more reliable for CeInCu₂.

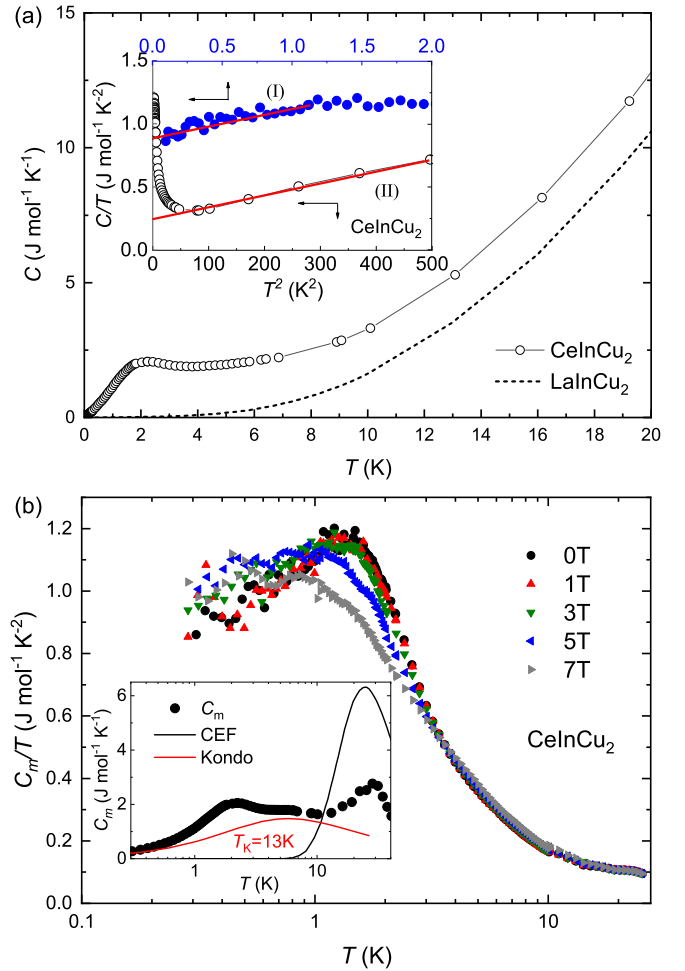


FIG. 7. (a) Specific heat $C(T)$ of CeInCu₂ and its nonmagnetic analog LaInCu₂. Inset shows C/T vs T^2 of CeInCu₂ in two low-temperature windows (curve I and II), from which γ_{LT} and γ_{HT} are estimated, see text. (b) Magnetic specific heat C_m divided by T , measured in varied fields, is shown as a function of temperature. Inset shows C_m vs T , and the calculated contributions of the Kondo effect and the CEF.

The $C_m(T)$ maximum at 30 K [Fig. 7(b) inset] is a Schottky anomaly arising from thermal population of the CEF states. A calculation based on the ground-state Kramers doublet and an excited quartet at $E_1 = 65$ K, which is in rough agreement with the CEF scheme determined from the inelastic neutron scattering [9], can qualitatively reproduce this anomaly. However, the calculated maximum is double the height of the measured one, manifesting a failure of the single-ion CEF picture due to the strong exchange effect as signified by the large value of $|\theta_p^{\text{HT}}|$, as well as the significant Kondo effect.

Different to CeInCu₂, NdInCu₂ shows a clear $C(T)$ peak at $T_N = 2.0$ K with, however, an extended high-temperature tail up to about 6 K that is indicative of strong critical fluctuation [Fig. 8(a)]. At $T < T_N$, C/T vs T^2 extrapolates linearly to $\gamma_{\text{LT}} = C/T (T \rightarrow 0) \approx 0.18 \text{ J mol}^{-1} \text{ K}^{-2}$ [Fig. 8(a) inset, curve I]. Applying field enhances the γ_{LT} value slightly and T_N shifts to lower temperature, different to the $T_N(B)$ variation observed in the magnetic measurement (Fig. 5). Given the absence of significant Kondo effect, the large γ_{LT} within the ordered phase

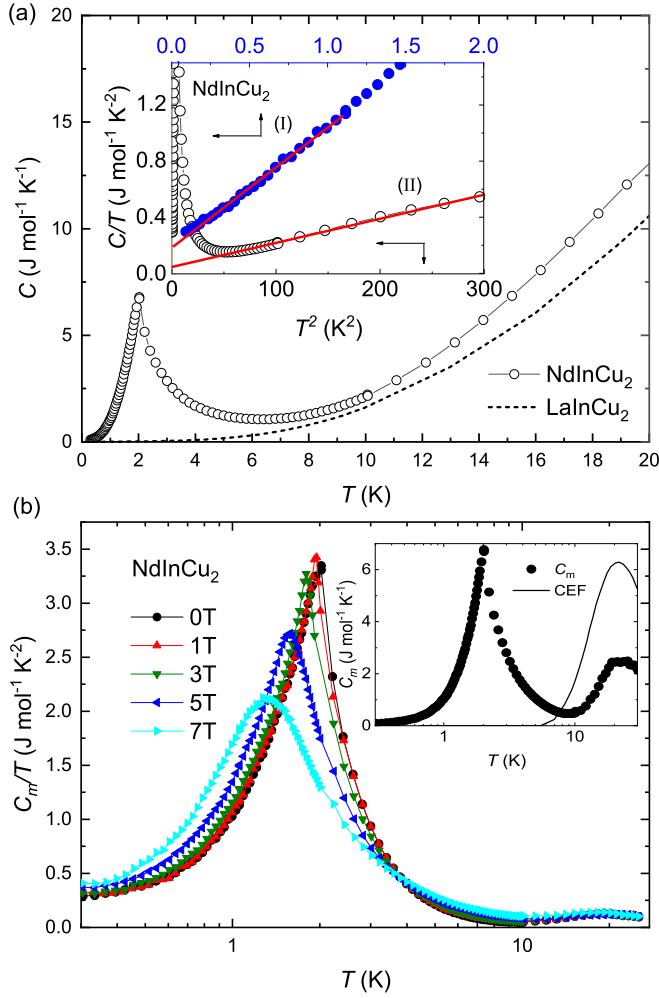


FIG. 8. (a) Specific heat $C(T)$ of NdInCu₂ and LaInCu₂. Inset shows C/T vs T^2 of NdInCu₂ in two low-temperature windows (curve I and II) to facilitate the estimation of γ_{LT} and γ_{HT} . (b) Magnetic specific heat divided by T , C_m/T , measured in varied fields. Inset shows $C_m(T)$ and the calculated Schottky anomaly, see text.

offers a straightforward manifestation of frustration-induced quantum fluctuation. In fact, enhanced linear-in-temperature specific heat at low temperature is an important hallmark of gapless quantum excitations in frustrated quantum magnets, even if no charge carriers are involved [25]. Alternatively, γ_{HT} estimated from the paramagnetic regime by extrapolating C/T vs T^2 linearly to 0 K [Fig. 8(a) inset, curve II] is $50 \text{ mJ mol}^{-1} \text{ K}^{-2}$, a value that is still sizable compared to that of LaInCu₂, $\sim 5 \text{ mJ mol}^{-1} \text{ K}^{-2}$. Like CeInCu₂, the two γ values of NdInCu₂ differ by a factor of about four. Furthermore, as shown in Fig. 8(b) inset, a broad Schottky anomaly shows up in $C_m(T)$ at around 22 K, and can be qualitatively reproduced by considering a ground-state Kramers doublet and two low-lying quartets at $E_1 = 57 \text{ K}$ and $E_2 = 480 \text{ K}$ (the Nd³⁺ multiplet with $J = 9/2$ in a cubic point symmetry is split into a doublet and two quartets). The calculated Schottky anomaly is much higher in height than the observed one, again indicating a partial failure of single-ion description of the CEF, in analogy to CeInCu₂.

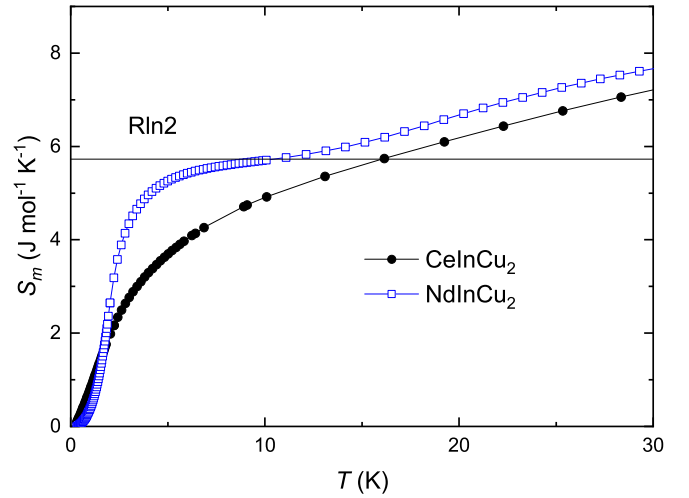


FIG. 9. Magnetic entropy S_m estimated from the magnetic specific heat for CeInCu₂ and NdInCu₂.

The magnetic entropy $S_m(T)$ computed by integrating C_m/T with respect to T is shown in Fig. 9. For CeInCu₂, S_m released at $T_N \approx 1.4 \text{ K}$ is only $0.22 \times R\ln 2$, strongly reduced from the entropy associated with a Kramers doublet by the Kondo effect and the spin frustration. Impressively, $S_m(T)$ does not saturate to $R\ln 2$ at any temperature but increases smoothly all the way, hinting at a substantial mixing between the CEF ground state and the low-lying multiplet, as reflected by the large value of $\mu_{\text{eff}}^{\text{LT}}$. For NdInCu₂, $S_m(T) = 0.46 \times R\ln 2$ at $T = T_N$ and it flattens out to $R\ln 2$ at 10 K that is five times the value of T_N , indicative of a Kramers doublet at the ground state and strong short-range spin correlations at $T > T_N$.

Magnetic phase diagram constructed from the magnetic and specific-heat measurements are shown in Fig. 10(a) and 10(b) for CeInCu₂ and NdInCu₂, respectively. For both compounds, T_N determined from $\chi(T)$ slightly increases upon applying small field, and after passing through a maximum around $B = 2 \text{ T}$, it starts to decrease smoothly until the critical

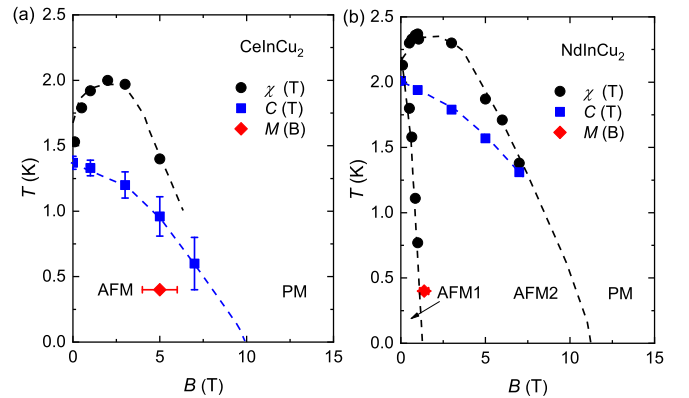
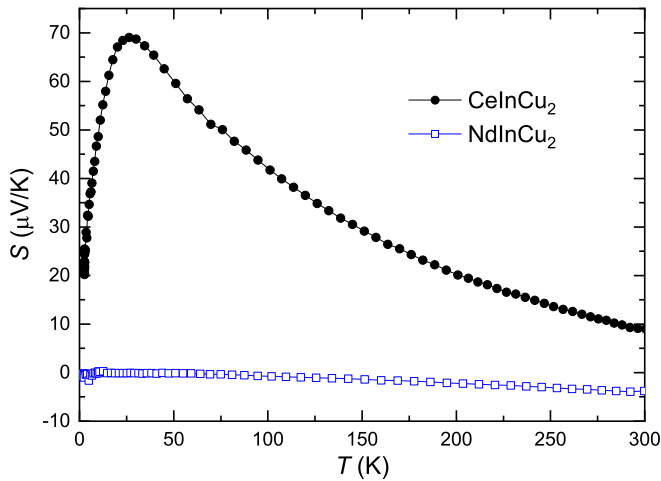
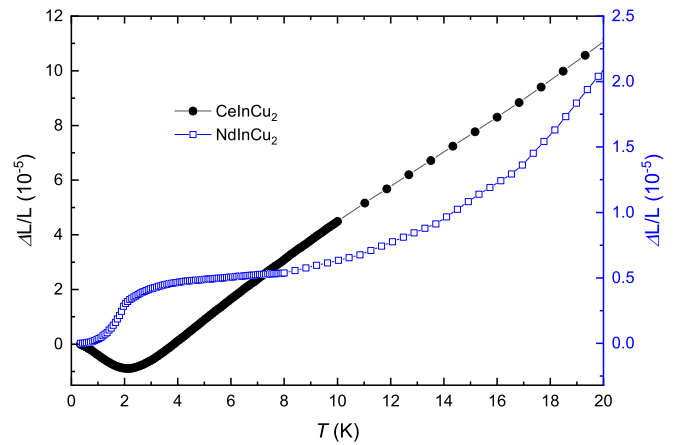


FIG. 10. Temperature-field magnetic phase diagram of CeInCu₂ (a) and NdInCu₂ (b) for $B \parallel [100]$. For NdInCu₂, the antiferromagnetic phase space is divided into two (AFM1 and AFM2) by the weak spin-flop transition, and a similar division in CeInCu₂ is also hinted by the data point (red diamond) determined by the weak incipient metamagnetic signature.

FIG. 11. The thermopower $S(T)$ of CeInCu₂ and NdInCu₂.

field near 10 T where $T_N \rightarrow 0$ takes place. The dome-like $T_N(B)$ profile at low fields shows significant discrepancy with that determined from the specific-heat measurement, which decreases smoothly and monotonically with field. For fields less than about 1 T, $\chi(T)$ of NdInCu₂ shows an additional drop at temperature below T_N , confirmed by the weak but well-defined metamagnetic transition [see Fig. 6(b) inset]. This causes a secondary antiferromagnetic phase in NdInCu₂ [AFM1 in Fig. 10(b)], whose phase boundary, however, cannot be probed by specific heat because very little entropy is involved. Likewise, for CeInCu₂, a weak incipient metamagnetic signature [Fig. 6(a) inset] within the antiferromagnetic phase is also observed, see the red data point in Fig. 10(a). The discrepancy between the T_N values determined from susceptibility and specific heat is a fingerprint of competing magnetic interactions and the subsequent short-range and dynamic antiferromagnetic correlations, as has been discussed for the frustrated CePdAl [26,27]: The dc susceptibility measures only the uniform spin susceptibility and is insensitive to the dynamic spin response, whereas the specific heat is able to thermodynamically probe dynamic spin correlations of various nature. In fact, $1/T_1T$ of CePdAl obtained from the NMR measurement, which is related to dynamic spin susceptibility, reveals a sharp peak at $T_N = 2.7$ K, in contrast to the broad maximum of dc susceptibility at 4 K [27].

Figure 11 displays the thermopower $S(T)$, which is strikingly different between the two compounds like the $\rho(T)$ profile. CeInCu₂ is characterized by a large $S(T)$ maximum at $T = 25$ K surmounting to 70 $\mu\text{V}/\text{K}$. It constitutes one of the largest thermopower values in heavy-fermion compounds at such a low temperature. The one-maximum $S(T)$ behavior of CeInCu₂, like its counterpart in $\rho(T)$, indicates significant contribution from thermal population of the low-lying CEF states, in addition to the Kondo effect. By contrast, $S(T)$ of NdInCu₂ is quasi-linear-in-temperature and remains less than 5 $\mu\text{V}/\text{K}$ in the whole temperature range investigated, typical of a simple metal without significant electron correlations. The Kondo physics is apparently not involved in NdInCu₂ albeit the enhanced C/T values at low temperatures. Interestingly, an even higher $S(T)$ maximum of 89 $\mu\text{V}/\text{K}$ at 25 K has ever been reported for a polycrystalline CeInCu₂ [13].

FIG. 12. Relative length change $\Delta L/L$ of CeInCu₂ and NdInCu₂ measured along the [100] direction.

The large thermopower of this compound, therefore, deserves further attention from the perspective of cryogenic thermoelectric application.

Figure 12 displays the relative length change $\Delta L/L$ vs T of the two compounds measured along [100]. Thermal expansion of CeInCu₂ has been studied previously [22,28]. These studies, however, have either used poly crystal or been performed down to only 2 K. Our measurements on single crystal down to lower temperatures reveal striking difference between the two homologs. The lattice of CeInCu₂ shows a broad minimum at $T \approx 2$ K with no definite signature of magnetic ordering but an obvious competition between large positive and large negative thermal expansion, whereas the lattice of NdInCu₂ shrinks evidently at T_N , preceded by an incipient lattice contraction due to short-range correlation from about 4 K.

The linear thermal expansion coefficient, defined as $\alpha = d(\Delta L/L)/dT$, is shown in Fig. 13(a) for both compounds. Literature data for polycrystalline CeInCu₂ are also shown for comparison [22]. After developing a broad maximum at around 4 K, $\alpha(T)$ of CeInCu₂ drops smoothly upon cooling and assumes a negative maximum at $T \approx 1$ K, considerably lower than $T_N = 1.4$ K determined from the C_m/T peak. A similar negative $\alpha(T)$ maximum has been frequently observed in Ce-based heavy-fermion compounds [29–32], signaling the competition between the Kondo effect and the RKKY interaction that is highly volume sensitive. Whether T_N can be pinpointed in $\alpha(T)$ strongly depends on the degree of the competition: Some materials show sharp $\alpha(T)$ drop at T_N , like in CeIn₃ [29], Ce₂RhIn₈ [30], and CePd₂Si₂ [31], whereas others only a broadened transition near T_N , as observed in CeInCu₂ and CePtSi₂ [32]. The smooth drop of $\alpha(T)$ from 4 K to 1 K across T_N in CeInCu₂, in contrast to the sharp anomaly at T_N observed in CeIn₃ that has similar energy scales of both the Kondo effect and the RKKY interaction, offers another signature of spin-frustrated antiferromagnetic interaction. Unlike CeInCu₂, $\alpha(T)$ of NdInCu₂ shows a clear peak at $T_N \approx 2$ K, resembling that of its $C(T)$ and no negative $\alpha(T)$ values are visible.

Thermodynamically, α probes entropy change of condensed matter in response to volume/length change, as

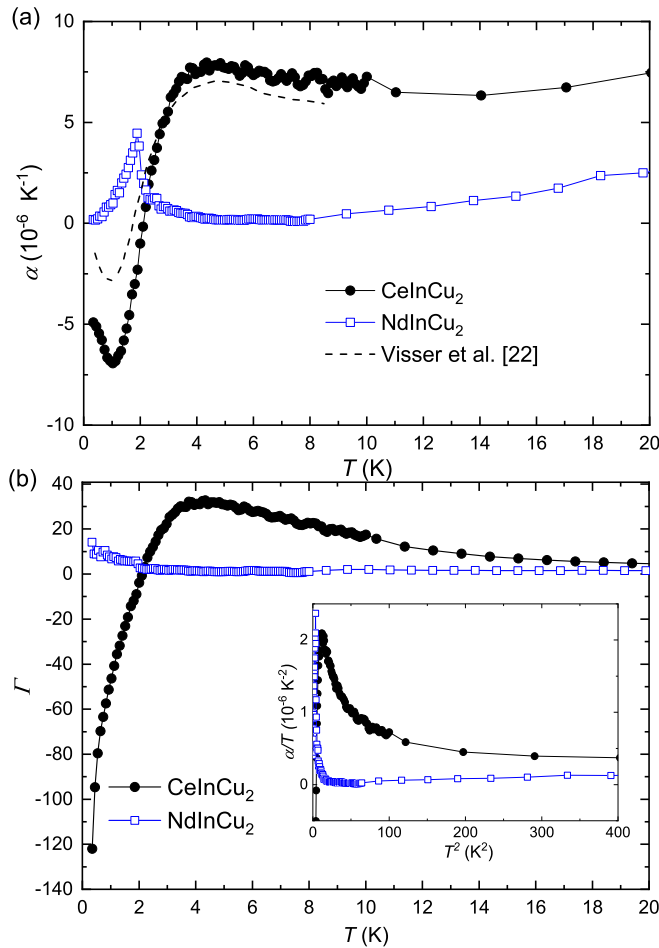


FIG. 13. (a) The linear thermal expansion coefficient $\alpha(T)$ of CeInCu₂ and NdInCu₂. Literature data for a poly crystal of CeInCu₂ are also shown for comparison. (b) The Grüneisen ratio Γ determined from the measured thermal expansion and specific heat. Inset shows α/T vs T^2 for the two compounds.

compared to its counterpart C , which detects entropy in response to temperature change. The distinct low-temperature $C(T)$ and $\alpha(T)$ profiles in CeInCu₂, in contrast to the more similar profiles of the two quantities in NdInCu₂, point to a highly volume-dependent thermodynamics in the former compound. Different volume effects of the two compounds can be better illustrated in α/T vs T^2 shown in Fig. 13(b) inset, where $\alpha/T(T^2)$ of NdInCu₂ traces approximately a linear function at $T > T_N$ that is similar to its C/T vs T^2 dependence [Fig. 8(a) inset]. By contrast, $\alpha/T(T^2)$ of CeInCu₂ at $T > T_N$ deviates largely from linearity and keeps on growing with cooling in a way that is very different from its $C/T(T^2)$ [Fig. 7(a) inset], suggesting a more singular thermal expansion than specific heat originating in the Kondo physics, but not spin frustration.

The distinct volume-dependent thermodynamics can be parameterized by the so-called Grüneisen parameter Γ defined through C and α , $\Gamma = B_T V_m \beta / C$, where B_T is the isothermal bulk modulus (55 GPa for CeInCu₂, see Ref. [28]) and $\beta = 3\alpha$ the volume thermal expansion coefficient. Intensive investigations on the Grüneisen parameter of Kondo-lattice compounds

[33] have revealed that Γ is generically greatly enhanced over unity that is expected for simple metals, and can serve as a unique quantity characterizing the strength of Kondo hybridization. Indeed, $\Gamma(T)$ of CeInCu₂ [Fig. 13(b)] becomes significantly large already at temperatures well above T_N in reflection of the strong volume dependence of the Kondo-derived electronic states. The sign change of $\Gamma(T)$ at low temperatures in CeInCu₂ marks the competition between the Kondo effect and the RKKY interaction: The former tends to delocalize the $4f$ electrons and favors smaller volume, whereas the latter prefers stable Ce^{3+} with larger volume. By contrast, $\Gamma(T)$ of NdInCu₂ is always positive and close to unity down to nearly T_N . Intriguingly, at $T < T_N$, $\Gamma(T)$ does not keep flat but goes up increasingly upon cooling. At $T = 0.3$ K, the lowest temperature of our measurement, Γ of NdInCu₂ attains a value as high as 10. In general, such a continuous enhancement of Γ towards $T = 0$ K indicates growing quantum fluctuation near a quantum critical point [33], where T_N is smoothly suppressed. The surprising existence of this singular $\Gamma(T)$ behavior in non-Kondo NdInCu₂ points to potential quantum critical fluctuation even in the ordered phase, in line with the unusually enhanced linear specific-heat coefficient γ_{LT} in this compound.

IV. DISCUSSION AND SUMMARY

Our detailed studies on CeInCu₂ and NdInCu₂ have revealed a number of similarities and distinctions between the two compounds. They both have a large paramagnetic Weiss temperature relative to their respective Néel temperature and consequently a large frustration ratio, as well as an enhanced electronic specific-heat coefficient γ . Impressively, similarities are observed in their phase diagrams, too. Here, the temperature of the $\chi(T)$ peak reveals a nonmonotonic field dependence and forms a broad dome over the T_N values determined from specific heat, and is eventually suppressed to zero at a critical field of ~ 10 T.

Comparability of the two compounds also lies in their Kadowaki-Woods (KW) ratio A/γ^2 (Fig. 14). The ratio, evaluated from the linear specific-heat coefficient deep in the ordered phase (γ_{LT}) is 0.75 and $1.17 \times 10^{-6} \mu\Omega \text{ cm K}^2 \text{ mol}^2 \text{ mJ}^{-2}$ for CeInCu₂ and NdInCu₂ (solid circles in Fig. 14), respectively. These are compared to the standard KW ratio (solid line) known for typical heavy-fermion compounds with Kramers doublet ground state (with degeneracy $N = 2$, see Refs. [34,35]). Analogous deviations of the measured KW ratios from the standard value indicate an enhancement of γ_{LT} beyond the Kondo hybridization. Interestingly, by employing γ_{HT} estimated from the paramagnetic regime, the standard KW ratio can be restored for both compounds, see open circles in Fig. 14. This lends naive support to the excessive contribution to the low-temperature specific heat arising from frustration-induced quantum fluctuation. Finally, it is interesting to note that a strongly reduced KW ratio has also been observed in quasi-one-dimensional Kondo lattice compounds CeAu₂In₄ [36], YbNi₄P₂ [37], and CeRh₆Ge₄ [38] with enhanced spin dimensional frustration. Therefore, spin frustration might be one general mechanism underlying the KW ratio deviation found in various materials [35].

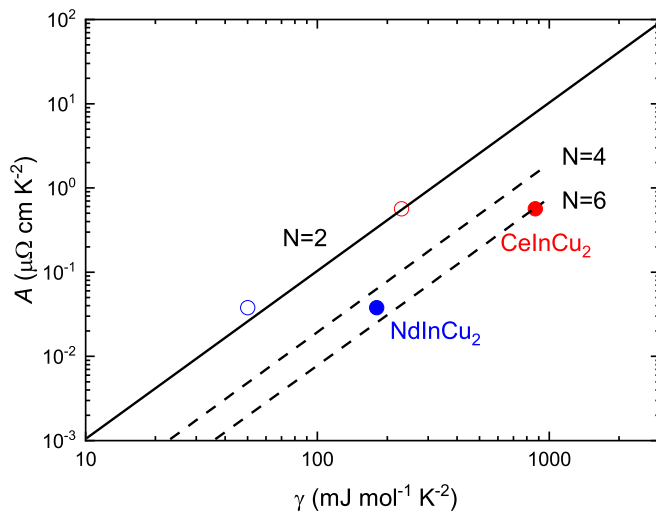


FIG. 14. The Kadowaki-Woods plot shown as a double-logarithmic relation of γ vs A for CeInCu_2 and NdInCu_2 . A solid line for typical Kondo intermetallics with doublet ground state ($N = 2$), $A/\gamma^2 \sim 10^{-5} \mu\Omega \text{ cm K}^2 \text{ mol}^2 \text{ mJ}^{-2}$, is shown for comparison. Note that the solid circles indicate the KW ratios with respect to γ_{LT} estimated from the ordered phase whereas the open circles are that with respect to γ_{HT} estimated from the paramagnetic phase. The dashed lines are theoretical expectation for ground-state degeneracy $N = 4$ and 6 , see Ref. [35].

The lack of significant Kondo effect in NdInCu_2 is apparent from its transport properties: Both the resistivity and thermopower are characteristic of simple metals, showing no Kondo-derived features despite its enhanced γ value. Unlike specific heat, definitive thermodynamic differences between CeInCu_2 and NdInCu_2 are observed in their thermal expansion coefficients: The Kondo physics is intimately related to the local-itinerant duality of the $4f$ electrons and is therefore much more susceptible to volume change than is the geometrical frustration. Nevertheless, spin frustration can influence low-temperature thermal expansibility as well as specific heat. For example, the Kondo temperature might be considerably underestimated if the low-energy spin dynamics stemming from frustration is left out. The newly estimated $T_K \approx 13$ K for CeInCu_2 based on the characteristic $C(T)$ hump is approximately double those in literature derived from either the $C/T(T \rightarrow 0)$ value or the entropy released at T_N . Moreover, the Grüneisen ratio of NdInCu_2 reveals an unexpected

increase in the ordered phase that is reminiscent of quantum critical fluctuation.

In summary, we have studied single crystalline CeInCu_2 and NdInCu_2 comparatively with competing physics among the Kondo effect, the RKKY interaction, and spin frustration in mind. Their magnetic phase diagrams share a striking similarity, which is seemingly irrelevant to Kondo physics, by showing a dome-like evolution of $T_N(B)$ determined from susceptibility that appears on top of the $T_N(B)$ profile from specific heat. The electronic specific-heat coefficient $\gamma = C/T$ ($T \rightarrow 0$) is enhanced in not only the Kondo intermetallics CeInCu_2 but also its non-Kondo counterpart NdInCu_2 . In particular, large zero-temperature C/T in the non-Kondo compound NdInCu_2 , which is higher than that of LaInCu_2 by orders of magnitude, points to significant quantum fluctuation in the ground state. The observed KW ratios deviate significantly from the standard value expected for Kramers doublet ground state. This ratio, however, can be restored for both compounds by considering the γ values extrapolated from the paramagnetic regime. The thermal expansibility appears to be the most distinct thermodynamic probe to discriminate the two compounds by showing large and sign-changing thermal expansion coefficient and Grüneisen ratio in CeInCu_2 that are rooted in the Kondo-derived $4f$ instability. These quantities are in fact also uncommon in NdInCu_2 , revealing a Grüneisen ratio that continuously increases upon cooling in the ordered phase, due most probably to the residual spin dynamics in the ground state. Given that a number of spin-frustrated Kondo systems have been demonstrated to show exotic ground-state quantum phase with non-Fermi liquid behavior, how the potential antiferromagnetic quantum criticality manifests itself differently in spin-frustrated non-Kondo intermetallics appears to be an interesting issue for future study.

ACKNOWLEDGMENTS

This work was supported by the National Natural Science Foundation of China (Grants No. 12141002 and No. 52088101), the National Key R&D Program of China (Grants No. 2022YFA1402200 and No. 2021YFA0718700), and the Chinese Academy of Sciences through the Project for Young Scientists in Basic Research (Grant No. YSBR-057), the Strategic Priority Research Program (Grant No. XDB33000000), and the Scientific Instrument Developing Project (Grant No. ZDKYYQ20210003). A portion of this work was carried out at the Synergetic Extreme Condition User Facility (SECUF).

- [1] G. R. Stewart, Heavy-fermion systems, *Rev. Mod. Phys.* **56**, 755 (1984).
- [2] P. Gegenwart, Q. Si, and F. Steglich, Quantum criticality in heavy-fermion metals, *Nat. Phys.* **4**, 186 (2008).
- [3] Q. Si, Quantum criticality and global phase diagram of magnetic heavy fermions, *Phys. Stat. Sol. B* **247**, 476 (2010).
- [4] P. Coleman and A. H. Nevidomskyy, Frustration and the Kondo effect in heavy fermion materials, *J. Low Temp. Phys.* **161**, 182 (2010).
- [5] H. Zhao, J. Zhang, M. Lyu, S. Bachus, Y. Tokiwa, P. Gegenwart, S. Zhang, J. Cheng, Y. Yang, G. Chen *et al.*, Quantum-critical phase from frustrated magnetism in a strongly correlated metal, *Nat. Phys.* **15**, 1261 (2019).
- [6] A. C. Y. Fang, S. R. Dunsiger, A. Pal, K. Akintola, J. E. Sonier, and E. Mun, Magnetic field induced effects in the quasikagome Kondo lattice system CePtPb , *Phys. Rev. B* **100**, 024404 (2019).
- [7] O. Stockert, J.-U. Hoffmann, M. Mühlbauer, A. Senyshyn, M. M. Koza, A. A. Tsirlin, F. M. Wolf, S. Bachus, P. Gegenwart,

- R. Movshovich, S. Bobev, and V. Fritsch, Magnetic frustration in a metallic fcc lattice, *Phys. Rev. Res.* **2**, 013183 (2020).
- [8] I. Felner, Magnetic and structural characteristics of the RInCu₂ compounds in the Heusler L2₁ structure, *Solid State Commun.* **56**, 315 (1985).
- [9] R. Lahiouel, J. Pierre, E. Siaud, R. M. Galera, M. J. Besnus, J. P. Kappler, and A. P. Murani, Kondo lattice and heavy fermions in Heusler phases: CeInAg_{2-x}Cu_x, *Z. Phys. B: Condens. Matter* **67**, 185 (1987).
- [10] R. Lahiouel, J. Pierre, E. Siaud, and A. P. Murani, Properties of CeInAg_{2-x}Cu_x Heusler phases, *J. Magn. Magn. Mater.* **63-64**, 104 (1987).
- [11] A. Najib, J. Beille, R. Lahiouel, and J. Pierre, Compressibility, thermal expansion and resistivity under pressure of the heavy fermion system CeInCu₂, *J. Phys. F: Met. Phys.* **17**, 2395 (1987).
- [12] S. Takagi, T. Kimura, N. Sato, T. Satoh, and T. Kasuya, Evidence for magnetic ordering in the heavy-electron compound CeCu₂In, *J. Phys. Soc. Jpn.* **57**, 1562 (1988).
- [13] S. Takayanagi, S. B. Woods, N. Wada, T. Watanabe, Y. Onuki, A. Kobori, T. Komatsubara, M. Imai, and H. Asano, Magnetic and transport properties in the cubic heavy fermion system CeInCu₂, *J. Magn. Magn. Mater.* **76-77**, 281 (1988).
- [14] H. Nakamura, Y. Kitaoka, K. Asayama, Y. Onuki, and T. Komatsubara, Successive magnetic transitions in the Heusler heavy-fermion system CeInCu₂, *J. Phys. Soc. Jpn.* **57**, 2276 (1988).
- [15] H. Kadowaki, S. Mitsuda, H. Yoshizawa, L. Rebersky, S. M. Shapiro, A. Kobori, Y. Onuki, and T. Komatsubara, Neutron scattering study of antiferromagnetic order in the heavy fermion CeInCu₂, *J. Phys. Soc. Jpn.* **58**, 4292 (1989).
- [16] N. Berry, E. M. Bittar, C. Capan, P. G. Pagliuso, and Z. Fisk, Magnetic, thermal and transport properties of Cd doped CeIn₃, *Phys. Rev. B* **81**, 174413 (2010).
- [17] J. X. Boucherle, J. Flouquet, Y. Lassailly, J. Palleau, and J. Schweizer, Magnetic form factor of cerium in the intermetallic compound CeIn₃, *J. Magn. Magn. Mater.* **31-34**, 409 (1983).
- [18] Y. Yamamoto and T. Nagamiya, Spin arrangements in magnetic compounds of the rocksalt crystal structure, *J. Phys. Soc. Jpn.* **32**, 1248 (1972).
- [19] K. Sato, Y. Isikawa, and K. Mori, Magnetic specific heat of light rare earth Heusler compounds RInCu₂, (R = La, Ce, Pr, Nd and Sm), *J. Magn. Magn. Mater.* **104-107**, 1435 (1992).
- [20] J. Arndt, N. Caroca-Canales, M. Dörr, C. Geibel, O. Stockert, and M. Loewenhaupt, Metamagnetic-like transition in the cubic heavy fermion compound CeIn_{3-x}Sn_x, *Physica C* **460-462**, 684 (2007).
- [21] T. Namiki, K. Nosaka, K. Tsuchida, Q. Lei, R. Kanamori, and K. Nishimura, Magnetic and thermal properties of NdT₂Al₂₀ (T: Ti, V, Cr) single crystals, *J. Phys.: Confer. Series* **683**, 012017 (2016).
- [22] A. de Visser, K. Bakker, and J. Pierre, Anomalous negative thermal expansion of CeInCu₂, *Phys. B: Condens. Matter* **186-188**, 577 (1993).
- [23] H. U. Desgranges and K. D. Schotte, Specific heat of the Kondo model, *Phys. Lett. A* **91**, 240 (1982).
- [24] V. T. Rajan, Magnetic Susceptibility and Specific Heat of the Coqblin-Schrieffer Model, *Phys. Rev. Lett.* **51**, 308 (1983).
- [25] S. Yamashita, Y. Nakazawa, M. Oguni, Y. Oshima, H. Nojiri, Y. Shimizu, K. Miyagawa, and K. Kanoda, Thermodynamic properties of a spin-1/2 spin-liquid state in a κ -type organic salt, *Nat. Phys.* **4**, 459 (2008).
- [26] H. Zhao, J. Zhang, S. Hu, Y. Isikawa, J. Luo, F. Steglich, and P. Sun, Temperature-field phase diagram of geometrically frustrated CePdAl, *Phys. Rev. B* **94**, 235131 (2016).
- [27] A. Oyamada, S. Maegawa, M. Nishiyama, H. Kitazawa, and Y. Isikawa, Ordering mechanism and spin fluctuations in a geometrically frustrated heavy-fermion antiferromagnet on the Kagome-like lattice CePdAl: A ²⁷Al NMR study, *Phys. Rev. B* **77**, 064432 (2008).
- [28] H. Matsui, T. Goto, T. Fujimura, Y. Onuki, T. Komatsubara, Y. Isikawa, and K. Sato, Magneto-acoustic effect of heavy fermion compound CeInCu₂, *J. Phys. Soc. Jpn.* **59**, 3451 (1990).
- [29] R. Schefzyk, M. Peschke, F. Steglich, K. Winzer, and W. Assmus, Thermal expansion study of magnetic phase transitions in Kondo-lattice systems, *Z. Phys. B: Condensed Matter* **60**, 373 (1985).
- [30] A. Malinowski, M. F. Hundley, N. O. Moreno, P. G. Pagliuso, J. L. Sarrao, and J. D. Thompson, Thermal expansion and magnetovolume effects in the heavy-fermion system Ce₂RhIn₈, *Phys. Rev. B* **68**, 184419 (2003).
- [31] N. H. van Dijk, B. Fak, T. Charvolin, P. Lejay, and J. M. Mignot, Magnetic excitations in heavy-fermion CePd₂Si₂, *Phys. Rev. B* **61**, 8922 (2000).
- [32] T. Nakano, G. Oomi, and T. Takeuchi, Thermal expansion and magnetostriction of the concentrated Kondo compound CePtSi₂, *J. Phys.: Conf. Ser.* **150**, 042139 (2009).
- [33] P. Gegenwart, Grüneisen parameter studies on heavy fermion quantum criticality, *Rep. Prog. Phys.* **79**, 114502 (2016).
- [34] K. Kadowaki and S. B. Woods, Universal relationship of the resistivity and specific heat in heavy-fermion compounds, *Solid State Commun.* **58**, 507 (1986).
- [35] N. Tsujii, H. Kontani, and K. Yoshimura, Universality in Heavy Fermion Systems with General Degeneracy, *Phys. Rev. Lett.* **94**, 057201 (2005).
- [36] M. Lyu, H. Zhao, J. Zhang, Z. Wang, S. Zhang, and P. Sun, CeAu₂In₄: A candidate of quasi-one-dimensional antiferromagnetic Kondo lattice, *Chin. Phys. B* **30**, 087101 (2021).
- [37] H. Pfau, R. Daou, S. Friedemann, S. Karbassi, S. Ghannadzadeh, R. Küchler, S. Hamann, A. Steppke, D. Sun, M. König, A. P. Mackenzie, K. Kliemt, C. Krellner, and M. Brando, Cascade of Magnetic-Field-Induced Lifshitz Transitions in the Ferromagnetic Kondo Lattice Material YbNi₄P₂, *Phys. Rev. Lett.* **119**, 126402 (2017).
- [38] B. Shen, Y. Zhang, Y. Komijani, M. Nicklas, R. Borth, A. Wang, Y. Chen, Z. Nie, R. Li, X. Lu, H. Lee, M. Smidman, F. Steglich, P. Coleman, and H. Yuan, Strange-metal behaviour in a pure ferromagnetic Kondo lattice, *Nature (London)* **579**, 51 (2020).